ASIA-PACIFIC NETWORK FOR GLOBAL CHANGE RESEARCH

Project Reference Number: ARCP2013-27NSY-Liu

The Impact of Global Warming on Ocean-Atmosphere Feedback Strength at the Tropical Indian Ocean

The following collaborator worked on this project:

1. Lin Liu (Project Leader), First Institute of Oceanography, State Oceanic Administration ,China, liul@fio.org.cn
2. Juneng Liew (Collaborator), National University of Malaysia, Malaysia, jnliew@gmail.com
3. Tim Li (Collaborator), University of Hawaii/International Pacific Research Center, USA, timli@hawaii.edu
4. Somkiat Khokiattiwont (Collaborator), Phuket Marine Biological Center, Thailand, skhokiattiwong@gmail.com
5. Shahbaz Mehmood (Collaborator), Global Change Impact Studies Centre, Pakistan, shahbaz.mehmood@gcisc.org.pk
6. Hussain Waheed (Collaborator), Maldives Meteorological Service, Maldives, husynwahyd@hotmail.com
7. Anna Kuswardani (Collaborator), Research and Development Centre for Marine and Coastal Resources, Indonesia. anastasia.tisiana@gmail.com

INTERNATIONAL PACIFIC RESEARCH CENTER

Project Refence Number: ARCP2013-27NSY-Liu

The Impact of Global Warming on Ocean-Atmosphere Feedback Strength at the Tropical Indian Ocean

Final Report Submitted to APN

Part One: Overview of Project Work and Outcomes

Non Technical Summary

With the scientific and financial support from APN, the participants of the project performed kinds of activities based on the proposed research program. The participants of the project conducted research activities in order to reveal the variability of air-sea interaction feedback strength under different projects, such as current and global warming scenarios. The results from the research activities had been published in the peer-reviewed journal and some of the results been cited by IPCC AR5. This project also held a workshop with the purpose of enhancing the internal communication among project staffs, specifically for the discussion of disseminating the project outcome into the public as well as the police makers. The representative from the Monsoon Onset Monitoring and its Social Economy Impact (MOMSEI) project, pilot project of Intergovernmental Oceanographic Commission /Sub-Commission for the Western Pacific (IOC/WESTPAC), agreed to cooperate with this project and invited the project leader to join the relevant scientific activities for better spreading the project outcome to different research groups as well as potential scientific users. This project also contributes to enhance the international marine cooperation between China and Maldives, Indonesia. The new project, titled as “The Java Upwelling dynamic and the relevant ecosystem variation (JUV)”, resulted from this project was supported for the next few years by SOA for better understanding the local climate variability over tropical Indian Ocean region, which will also give relative contribution to International Indian Ocean Expedition – 2 programs.

Keywords

Tropical Indian Ocean, air-sea interaction, Indian Ocean Dipole, dynamic feedback, thermodynamic feedback

Objectives

The main objectives of the project are
1. To conduct a detailed analysis to assess the variability of the dynamic and thermodynamic feedback strength associated with IOD under current and global warming scenario.
2. To setup the potential pathway to cooperated with other international project under IOC as well as other platform.
3. To introduce the new methodology to evaluate the simulated variability of the dynamic and thermodynamic feedback strength associated with IOD.
4. To disseminate the research outcome to relevant research groups as well as other potential scientific users, especially to the numerical modeling developer for further improve the numerical model simulation at tropical Indian Ocean region.

Amount Received and Number of Years Supported

The Grant awarded to this project was:

US$ 23,300 for 1 Year

Notes: 80% of the total amount awarded, the total amount is $29,000

Activity Undertaken

- Conducted the research activities on air-sea feedback strength under the historical and future projection based on CMIP5 multimodel outputs.
- Held the workshop in The Tianfu sunshine Hotel at Chengdu, China during 16-18 August 2014
- Disseminated the related result in different ways:
  1. Pan-CLIVAR conference workshop in Hague, Netherland, 14-19 July 2014.
  2. MOMSEI summer school in Jakarta, Indonesia, 8-13 September 2014.
  3. Workshop of joint project Java Upwelling variability at Qingdao, China on 12-14, December 2013.
  4. Second planning workshop of “Eastern Indian Ocean Upwelling Research Initiative (EIOURI)” at Qingdao, China on 21-22 November 2013.
  5. CLIVAR/Indian Ocean Panel-Pacific Panel joint conference at Lijiang, China on 8-10 July 2013.
- Training activities for Kenya young researcher.
- Discussed with the experts and representative from MOMSEI project, which is the pilot project of IOC/WESTPAC, for the future cooperation for the better cooperation.
- Proposed new project, titled as “The Java Upwelling dynamic and the relevant ecosystem variation”, supported by SOA
- Help build up the marine cooperation between China and Maldives, Indonesia.

Results

1. Scientific research
   1) Identify the dynamic feedback and thermodynamic feedback strength in historical simulation from CMIP5. Although most of CMIP5 coupled models could reproduce the IOD-like events and relevant dynamic and thermodynamic feedback processes in the tropical IO, unreasonable simulations exist among these models. The shortwave radiation-SST feedback is the important thermodynamic air-sea coupling process that could impact the IOD strength.
   2) In response to increased greenhouse gases, an IOD-like warming pattern appears in the equatorial Indian Ocean, with shoaling thermocline and strengthened thermocline feedback in the eastern equatorial Indian Ocean, the interannual variance of the IOD mode remains largely unchanged in sea surface temperature (SST) as atmospheric feedback and zonal wind variance weaken under global warming.

2. Cooperation with other international project and association
   1) The MOMSEI project, pilot project of IOC/WESTPAC, agreed to cooperate with this project and also adopted the relevant research outcome for its in-situ observation plan modification, since APN project identified the key area of the upwelling system for the tropical Indian Ocean variation, which is also one of the major concerns of MOMSEI project.
   2) This new project builds up the bridge with Eastern Indian Ocean Upwelling Research Initiative (EIOURI) project for IIOE-2 programs. As one of the research foci of CLIVAR, Indian Ocean upwelling events and their environmental impact set up the challenge for the local marine and climate variations. The EIOURI project also invited some of our project participants to work together in the quite near future.

Relevance to the APN Goals, Science Agenda and to Policy Processes

Tropical Indian Ocean air-sea coupled event is the most important interannual phenomena, which modulate the variation of Asian summer monsoon system. The influence from global warming to inner air-sea feedback strength of tropical Indian Ocean air-sea coupled event is still unclear and is one of challenge for relevant research. The result of this project will benefit to understand the internal mechanism relevant to Indian Ocean air-sea interaction events.

Self-evaluation

This project achieves the original research goals generally while there still lies in some insufficiency during the project performing.

Although our project got some results, which is rather preliminary and should be paid more attention, there still be long way for the better understanding these issues. One year time is too tight to complete all of the research.

Potential for further work

We are going to continue the data preparation for the further analysis based on the methodology introduced by the project. Previous studies describe the detailed information for the scientific research, while, the relevant communication among different projects and other international associations will be the most important activities we should strengthen in the future. As we mentioned before, the project outcome presents the importance of the upwelling for IOD simulation, which is also one of the major concern of CLIVAR as upwelling is one of the research foci in the future for CLIVAR level. Based on our finding, EIOURI project invited the participants of this project to join and contribute to IIOE-2 in the quite near future.

After the communication and discussion with the representative, the pilot project of IOC/WESTPAC, MOMSEI, has agreed to work together, which will be a good opportunity for disseminating our project into more persons and organization. The proponents will try the best to enhance the communication with IOC/WESTPAC for the further cooperation. Also, we will build the connection with numerical model developer in order to improve their coupled models based on our research.

Publications

1. Lin Liu, Shang-Ping Xie, Xiao-Tong Zheng, Tim Li,Yan Du, Gang Huang and Wei-Dong Yu,2013: Indian Ocean variability in the CMIP5 multi-model ensemble: The Zonal Dipole mode, Climate Dynamics. DOI: 10.1007/s00382-013-2000-9

2, Zheng, X.-T., S.-P. Xie, Y. Du, L. Liu, G. Huang, and Q.-Y. Liu, 2013: Indian Ocean Dipole response to global warming in the CMIP5 multi-model ensemble. J. Climate. doi: http://dx.doi.org/10.1175/JCLI-D-12-00638.1

Acknowledgments

Bedsides the support on both finance and scientific scope from APN, our work also has been supported by MOMSEI project from IOC/WESTPAC. We also appreciate the support from Dr. Weidong YU co-chair of IOC/WESTPAC Indian Ocean Panel.

We appreciate Dr. Xiaotong Zheng from Ocean University of China, Dr. Shangping Xie from Scripps Institute of Oceanography, U. S. for their joint effort and great contribution to this project.

Preface

Indian Ocean Dipole is a significant ocean-atmosphere coupled event over the tropical Indian Ocean. It is largely controlled by internal air-sea feedback mechanisms and strongly modulating the Asian climate variability, locally and remotely. Global warming is the apparent climatic long term trend over the globe, including the Indian Ocean region. This project examines the impact of global warming on this ocean-atmosphere coupled event using the CMIP5 output. Particularly the output answers the questions 1) to what degree the global warming impacts the IOD event and 2) to explain the physical mechanism on how the IOD is influenced by the global warming.

Table of Contents

1. Introduction

The Indian Ocean Dipole (IOD) is a basin-scale ocean-atmosphere coupled mode, characterized by a zonal contrast of a positive and a negative SST anomaly (SSTA) along the equatorial Indian Ocean (IO) and a zonal wind anomaly over the central equatorial IO. During a positive IOD event, the SST is anomalously cool in the southeastern IO (SEIO) off Sumatra) and warm in the western IO (WIO), accompanied with pronounced anomalous southeasterlies along the coast of Sumatra and anomalous easterlies over the central equatorial IO (CEIO). While the IOD rapidly develops in boreal summer, it reaches a mature phase in northern fall. A number of studies showed that the convection associated with IOD exerted a great impact on climate variability in Africa, South Asia, East Asia, and other remote regions It was suggested that Bjerkness feedback may operate in the equatorial IO. This dynamic feedback involves interactions among the zonal SST gradient, low level wind

in the CEIO, and the east-west thermocline displacement. For example, a negative SSTA off Sumatra would induce anomalous low-level easterlies in the CEIO, which depress (lift) the thermocline to the west. The lifted thermocline to the east may enhance the SST cooling through the upwelling of anomalous cold subsurface water. The enhanced surface cooling further amplifies the easterly anomaly. Through this positive dynamic feedback, IOD develops. Previous study suggested that because of the strong seasonal variability of the monsoon winds, conditions are favorable for the Bjerkness feedback during the summer and early fall in IO, sometimes leading to the development of an IOD event. In addition to the dynamical coupling, the thermodynamical air-sea feedback also played a role during IOD development. Different from the Pacific El Nino during which there is a spatial phase difference between convection and SST anomalies, the SST and cloud anomalies are in general in phase in the tropical IO. This implies a stronger cloud radiation- SST negative feedback in IO. Another notable feature during IOD development is a season-dependent wind-evaporation-SST feedback. A pronounced south-easterly mean flow in boreal summer leads a positive wind-evaporation-SST feedback, that is, a cold SSTA in the SEIO forces a low-level anticyclonic flow to the west of the anomalous heat source, and anomalous south-easterlies along the coast of Sumatra associated with this anticyclone strengthen the surface evaporation and cool the SST further. As the seasonal prevailing wind switches from south-easterlies in boreal summer to north-westerlies in boreal winter, this SST-wind-evaporation feedback becomes a negative one. Li (Li et al, 2003) suggested that this season-dependent thermodynamic air-sea feedback is responsible for the occurrence of the maximum SSTA in the SEIO in northern fall. The strength of the dynamic and thermodynamic feedbacks mentioned above depends greatly on the mean state of the tropical IO. For example, the mean thermocline depth and the background vertical velocity and vertical temperature gradient are critical in determining the effect of the dynamic feedback. A deeper mean thermocline, a smaller mean upwelling velocity and a weaker upper-ocean vertical temperature gradient may reduce heat exchange between the subsurface and surface. As discussed above, the wind-evaporation-SST feedback also depends on the background monsoon flow. In addition, the background vertical shear in boreal summer may promote a more equatorially symmetric wind response to an asymmetric SSTA forcing in the eastern IO. The enhanced symmetric response may strengthen the zonal wind at the equator and thus enhance the Bjerkness dynamic feedback. In this project, we explore the modification in the aforementioned feed-back processes under the pressure of a warming climate.

2. Methodology

2.1 Datasets

The primary datasets used for this study are the outputs of available models from the WCRP CMIP5 datasets. The model variables used in the diagnosis include 3D ocean temperature, current, surface wind, cloud fraction, specific humidity, and surface heat flux fields. Further detailed information can be obtained by checking the following website: (http://cmip-pcmdi.llnl.gov/cmip5).

The particular datasets analyzed here are so-called Climate of the Twentieth-Century Experiment (20c3M) (historical run) for current study. The forcing agents of this experiment include greenhouse gases (CO2, CH4, N2O, and CFCs), sulphate aerosol direct effects, volcanoes, and solar forcing (Taylor et al. 2012). The results reported in this analysis were

only for the period between January 1950 and December 1999 in order to compare with the observational datasets. The mean climatological annual cycle was defined based on this 50-year period. The interannual anomalies were then obtained by subtracting the monthly mean variables from their respective mean climatological annual cycles. For the future projection, we analyze two sets of simulations (Taylor et al. 2012): 106-year simulations forced by historical greenhouse gases (GHG), aerosols and other radiative forcing from 1900 to 2005; 95-year projections under the RCP8.5 scenario from 2006 to 2100, with the radiative forcing reaching ~ 8.5 W m-2 near 2100 (equivalent to > 1370 ppm CO2 in concentration). In this study we also use outputs from 17 models, including SST, sea surface height (SSH), surface wind, precipitation, and sea water temperature. In each model, the initial conditions for the RCP8.5 experiment are taken from 1 January 2006 of the historical experiment. So here we combine the two experiments to form a 201-year-long dataset and examine the TIO mean state change and IOD response to global warming.

For comparison of the model simulations with the observations, various observed and reanalyzed (assimilated) atmospheric and oceanic datasets were used. Three-dimensional atmospheric wind fields, the surface specific humidity, the surface latent heat flux, and the net surface short wave radiation were obtained from the National Centers for Environmental Prediction and the National Center for Atmospheric Research (NCEP/NCAR) reanalysis product (Kistler et al. 2001), and three-dimensional ocean temperatures were obtained from the Simple Ocean Data Assimilation (SODA) reanalysis (Carton et al. 2000). Cloud fraction is taken from ECMWF 40-Year Re-analysis Data. In addition, we used the Hadley Centre Global Sea Ice and Sea Surface Temperature (HadISST) product (Rayner et al. 2003). Most of the observed or reanalysis datasets were available for the 50-yr period (from January 1950 to December 1999).

2.2 The measurement of feedback index

This project focused on the scientific research on the air-sea feedback strength (Fig. 1) in associated with the Indian Ocean Dipole model variability simulated by CMIP5 models under different projections. The major methodology used in this project is providing the feedback index measuring kinds of dynamic and thermodynamic feedback strength quantitatively.

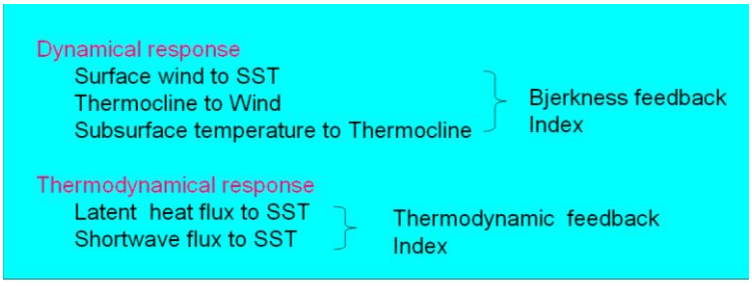

Figure 1. The diagram of the dynamic and thermodynamic feedback index components

We first examine the Bjerknes feedback strength in CMIP3 models. This dynamic air-sea coupling consists of three processes. The first is how the atmospheric low-level wind

responds to the SSTA forcing in the SEIO. It is well known that during the IOD development period (JAS), the most significant feature of SSTA is the dipole pattern. Such a zonal SSTA gradient causes a zonal wind response in the CEIO through the SST-gradient-induced pressure gradient in the atmospheric planetary boundary layer (Lindzen and Nigam 1987) or the mid-tropospheric heating anomaly (Gill 1980).

To quantitatively measure the strength of the zonal wind response to the SSTA, we first plot a scatter diagram for each model. Figure 2 shows the relationship between the SSTA in the SEIO (90-110oE, 10oS-0) and the zonal wind anomaly in the CEIO (70-90oE, 5oS-5oN) from the CMIP models. For comparison, the observed SST-wind relation is also plotted in the top left corner. Consistent with the observed relationship, all of the models exhibit a positive correlation between the zonal wind and SST anomalies, that is, a negative SSTA in the SEIO (which corresponds to a positive IOD event according to Saji et al. 1999) is accompanied with an easterly anomaly in the CEIO.

We hereby denote a SST-wind coupling coefficient, R(u, T), to represent how strong the low-level wind responds to a unit SSTA forcing at each model. Mathematically, it equals to the linear slope at each of scatter diagrams in Fig. 2. (The linear slope in all scattering diagrams was calculated based on the least square fitting method.) It is interesting to note that the averaged slope in the strong composite is about 2.2 m s-1 K-1, which is a little larger than the averaged slope (1.7 m s-1 K-1) in the weak composite. Compared to the observed R(u, T), the SST-wind coupling coefficient in the strong group appears more realistic.

The second process involves how the ocean thermocline responds to the equatorial surface wind forcing. The zonal wind anomaly in the CEIO in general forces two types of the ocean thermocline response, a fast adjustment in which the thermocline depth anomaly is approximately in a Sverdrup balance with the zonal wind stress anomaly, similar to that in the Pacific (Neelin 1991), and a slow evolution that involves the propagation of oceanic Rossby and Kelvin waves (Li et al. 2002, 2003; Yu et al. 2005).

Figure 3 shows the scatter diagrams between the zonal wind anomaly in the CEIO and the thermocline depth anomaly in the SEIO for each model. The observed feedback relation between the wind and SEIO thermocline depth anomaly is positive because an easterly wind anomaly in the CEIO may lift (suppress) the thermocline in the eastern (western) part of the basin. Such a positive relationship is captured by all of the coupled models.

We hereby denote a wind-thermocline coupling coefficient R(D, u) to measure the strength of thermocline depth change for a given unit zonal wind forcing. It can be represented by the slope in Fig. 3. The averaged R(D, u) for the strong composite is 4.2 m per ms-1, while it is about 2.9 m per ms-1 for the weak composite. The observed R(D, u) is somewhere between the values of the strong and weak composites.

The third process involves how the ocean subsurface temperature responds to the ocean thermocline variation. In the SEIO, a shoaling (deepening) of the thermocline leads to a negative (positive) temperature anomaly at a fixed subsurface level. The change of the subsurface temperature may further affect SST through the anomalous vertical temperature advection by the mean upwelling. In the region of deep climatological mean thermocline, the subsurface temperature variation is small, and so is the SST variability.

Figure 4 shows the observed and the model simulated relationship between the thermocline depth anomaly and the temperature anomaly at 70 m (where the subsurface temperature variability is largest, Hong and Li 2010) in the SEIO. A positive correlation appears between

the observed thermocline depth and subsurface temperature. We hereby denote R(Te, D) as a thermocline-subsurface temperature coupling coefficient, which can be measured by the slope in Fig. 4. The observed slope is 0.1 K m-1, implying that one meter thermocline change would lead to a subsurface temperature change of 0.1K.

The overall Bjerknes dynamic feedback strength should be determined by the combined effect of the three processes above. To quantitatively measure the Bjerknes feedback intensity and to compare it with the thermodynamic feedback intensity, we introduce a simplified SST tendency equation as below:

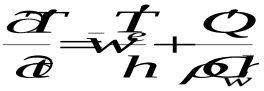

(1)

where T' and T_e' denote the surface and subsurface ocean temperature anomalies respectively, $\bar{w}$ denotes the climatological mean vertical velocity at the base of the ocean mixed layer, Q' is the net surface heat flux anomaly, ρ and C_w are the sea water density and specific heat, and h is the ocean mixed layer depth. In Eq. (1), we only show the thermocline feedback and heat flux terms and have neglected other advection terms for simplicity. Assuming $T' = \delta T e^{\sigma t}$, Eq. (1) may be rewritten as:

(2)

Here the left hand side of Eq. (2) is proportional to the growth rate (σ) of the SSTA. The second term in the right hand side of Eq. (2) represents how strong the surface heat flux anomaly is in response to a unit SSTA change. Thus it reflects the strength of the thermodynamic air-sea feedback. The first term in the right hand side of Eq. (2) represents the vertical advection of anomalous subsurface temperature by the mean upwelling velocity, thus reflecting the strength of the Bjerknes dynamic air-sea feedback. We hereby define the first term in the right hand side of Eq. (2) as the Bjerknes feedback intensity index (BFI) and the second term as the thermodynamic feedback intensity index (TFI). The BFI may be written as:

(3)

Equation (3) states that the BFI depends on the mean vertical velocity and a product of the SST-wind, wind-thermocline and thermocline-subsurface temperature coupling coefficients during the IOD developing phase. It measures the overall strength of the Bjerknes feedback in each model. Figure 5 shows the averaged values of the SST-wind, wind-thermocline and thermocline-subsurface temperature coupling coefficients and BFI respectively for the strong, moderate and weak composites. For comparison, the observed coupling coefficients and BFI are also shown in the figure. Note that the BFI is consistent with the overall strength of the IOD simulations, with the greatest (smallest) value occurring in the strong (weak) composite.

The above analysis points out the important role of the dynamic air-sea coupling in determining the strength of the model IODs.

To quantitatively measure the feedback strength, we plot the scatter diagram (Fig. 6) to illustrate the relationship between the surface latent heat flux (LHF) anomaly and the SSTA in the SEIO in JAS. For the comparison, the observed counterpart is also plotted.

We hereby denote R(LHF, T) to represent the SST-evaporation feedback coefficient, which can be measured by the slope at each panel of Fig. 6. The observed feedback coefficient is 8.1W m-2 K-1, which implies that for given 1K SST cooling, the resulting latent heat flux anomaly is 8.1 W m-2. This amount of anomalous heat flux could be used to further enhance the local SST cooling.

To illustrate how different the cloud-radiation-SST feedback is among the CMIP models, we show in Fig. 7 the simultaneous relation between the shortwave radiation and SST anomalies averaged in JAS over the SEIO. Different from the positive wind-evaporation-SST feedback, a negative feedback between the observed SST and shortwave radiation anomalies exists in the SEIO.

We hereby denote R(SWR, T) to measure the strength of the negative cloud-radiation-SST feedback. The averaged slope for the strong composite is -14 W m-2 K-1, which is about twice as large as that (-7 W m-2 K-1) in the weak composite.

The overall thermodynamic feedback intensity (TFI) may be measured by the sum of the wind-evaporation-SST feedback and the cloud-radiation-SST feedback, that is,

(4)

Figure 8 shows the diagrams of R(LHF, T), R(SWR, T) and TFI for the strong, moderate and weak composites and for the observation. The major bias appears in the latent heat flux-SST relationship. Consequently, the overall thermodynamic damping in all the three groups is overestimated, compared to the observation. The strongest (weakest) thermodynamic damping appears in the strong (weak) group.

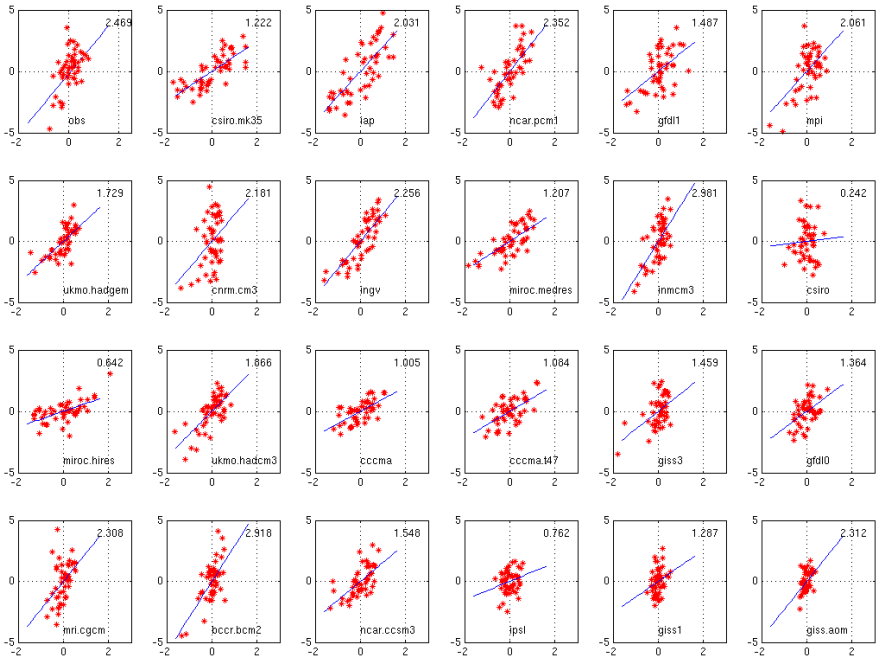

Figure 2. Scatter diagram between central Indian Ocean 850hPa zonal wind anomaly and the eastern SSTA for observation and each model during JAS. The number within each sub-figure is the slope of fitted line.

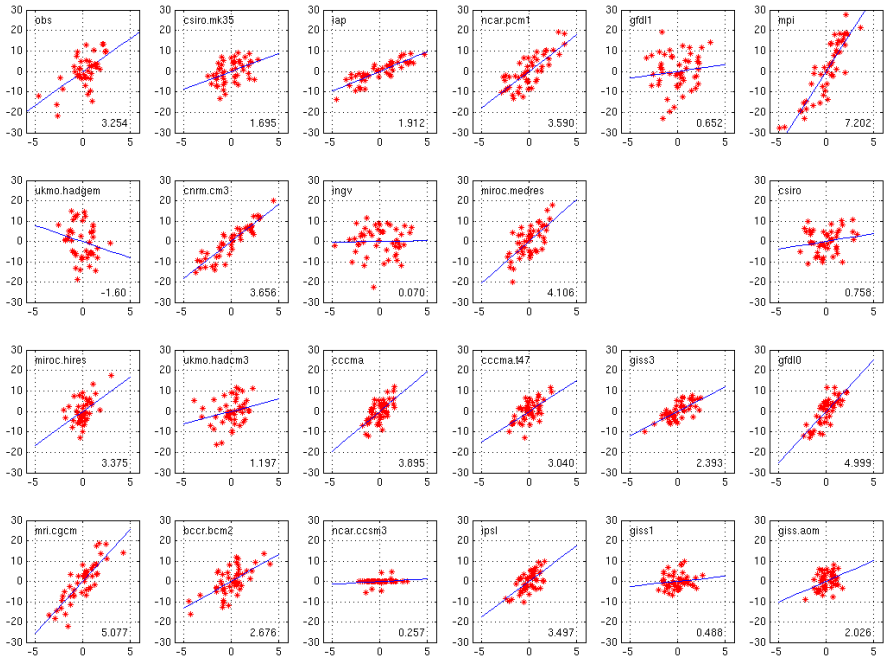

Figure 3. Scatter diagram between eastern IO thermocline depth anomaly and central Indian Ocean 850hPa zonal wind anomaly for observation and each model during JAS. The number within each sub-figure is the slope of fitted line.

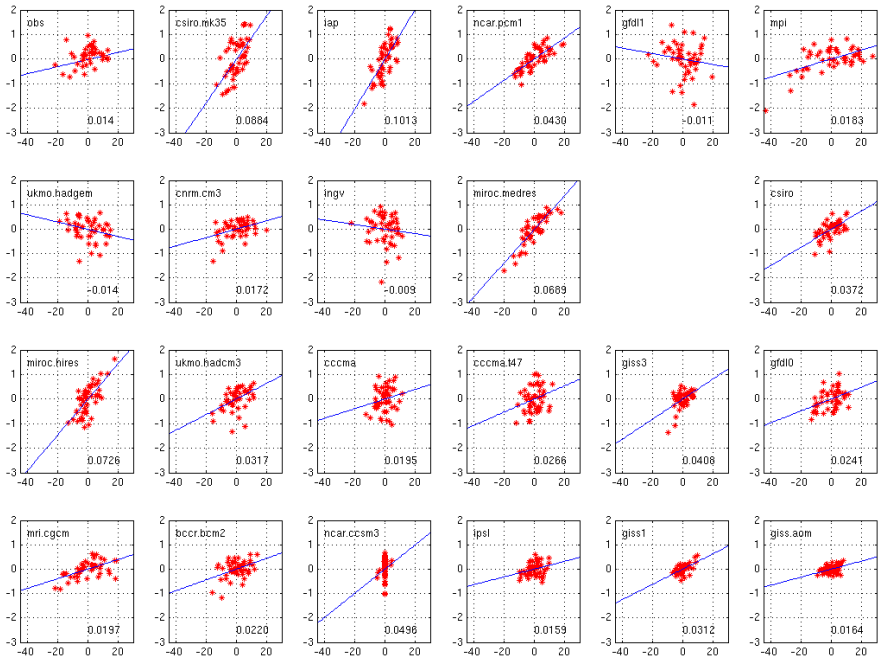

Figure 4. Scatter diagram between eastern SSTA and eastern IO thermocline depth anomaly anomaly for observation and each model during JAS. The number within each sub-figure is the slope of fitted line.

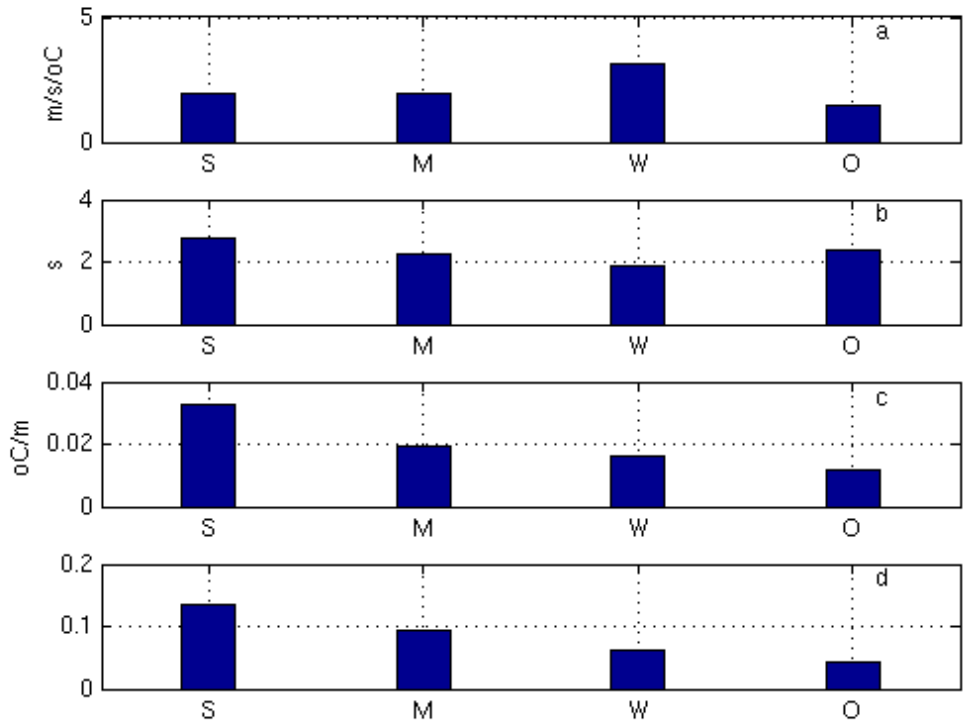

Figure 5. Separate and averaged BFI for the strong, moderate, weak composites and observation in JAS. (a) response of zonal wind anomaly to SSTA, (b) response of thermocline depth anomaly to zonal wind anomaly, (c) response of SSTA to thermocline depth anomaly, (d) averaged BFI. S, M, W, O at horizontal axis present strong, moderate, weak simulation models and observation.

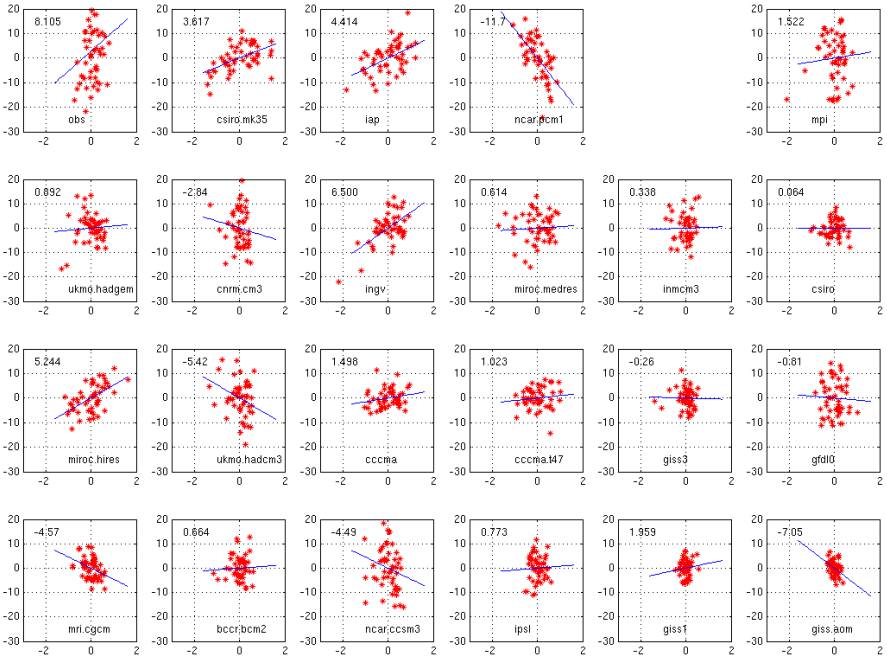

Figure 6 Scatter diagram between latent heat flux and SSTA over eastern Indian Ocean area for observation and each model during JAS. The number within each sub-figure is the slope of fitted line.

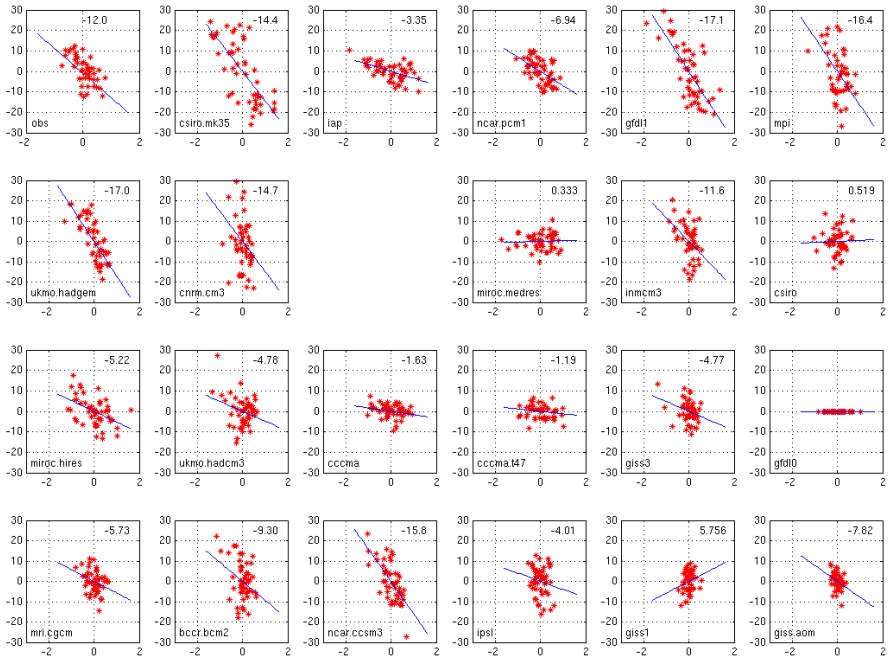

Figure 7. Scatter diagram between shortwave radiation anomaly and SSTA over eastern Indian Ocean area for observation and each model during JAS. The number within each sub-figure is the slope of fitted line.

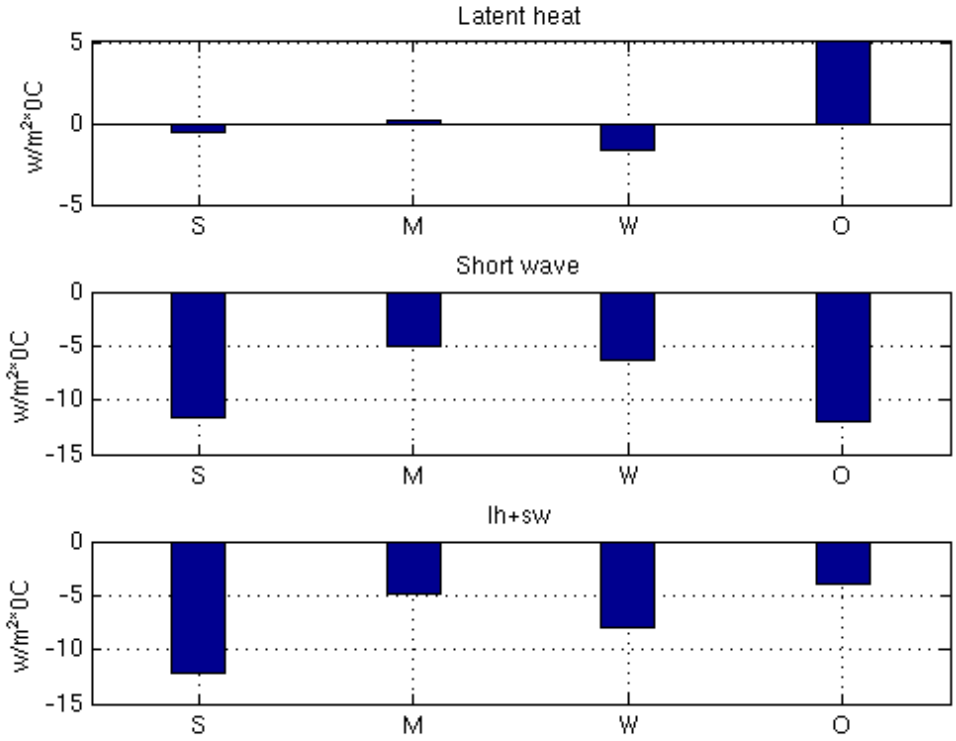

Figure 8 Separate and averaged thermodynamical index(TI) for the strong, moderate, weak composites and observation in JAS over eastern Indian Ocean. (a) response of latent heat flux anomaly to SSTA, (b) response of shortwave radiation anomaly to SSTA, (c) averaged thermodynamical index

3. Results & Discussion

3.1 Historical scenario

The composite results illustrate a remarkable difference in the zonal wind, SST and thermocline depth anomalies between the strong and weak groups (Figure not shown). Why do different model simulate the IOD strength differently and which air-sea coupling processes contribute to the difference? Previous research had pointed out that the dynamic and thermodynamic coupling strength of each model during the developing phase in July-August-September (JAS) were responsible for the diversity simulated IOD strength (Liu et al. 2011). Here, we present the detailed analysis for historical experiment from CMIP5 models.

a) Dynamic feedback

Figure 9 shows the relationship between the SSTA in the SEIO and the zonal wind anomalies in the CEIO from the 21 models. For comparison, the observed SST-wind relationship is plotted in each subplot. Consistent with the observed relationship, all of the models exhibit a positive correlation between the zonal wind and SST anomalies, that is, a negative SSTA in the SEIO (which corresponds to a positive IOD event according to Saji et al. (1999)) is accompanied with an easterly anomalies in the CEIO.

We hereby denote a SST-wind coupling coefficient, R(u, T), to represent how strong the low-level wind responds to a unit SSTA forcing at each model. Mathematically, it equals to the linear slope in each of scatter diagrams in Fig. 9, calculated based on the least square fitting method. It is interesting to note that the averaged slope in the strong composite is about 1.7 m s-1 K-1, much larger than the averaged slope (1.0 m s-1 K-1) in the weak composite. Compared to the observed R(u, T), the SST-wind coupling coefficient in the strong group appears more realistic.

The second process of Bjerknes feedback involves how the ocean thermocline responses to the equatorial surface wind forcing. Figure 10 shows the scatter diagrams between anomalies of zonal wind in the CEIO and the thermocline depth in the SEIO for each model. The observed feedback relationship between the wind and SEIO thermocline depth is positive because an easterly wind anomaly in the CEIO may lift (suppress) the thermocline in the eastern (western) part of the basin. Such a positive relationship is captured by all of the coupled models.

We denote a wind-thermocline coupling coefficient R(D, u) to measure the strength of thermocline depth change for a given unit zonal wind forcing. It can be represented by the slope in Figure 10. The averaged R(D, u) for the strong composite is 4.9 m per m s-1, while it is about 6.3 m per m s-1 for the weak composite. The observed R(D, u) is weaker than either of Bjerknes feedback values.

The third process involves how the ocean subsurface temperature responds to the ocean thermocline variation. In the SEIO, a shoaling (deepening) of the thermocline leads to a negative (positive) temperature anomaly at a fixed subsurface level. The change of the subsurface temperature may further affect SST through the anomalous vertical temperature advection by the mean upwelling. In the region of deep climatological mean thermocline, the subsurface temperature effect is small on SST variability.

Figure 11 shows the observed and the simulated relationship between anomalies of the thermocline depth and the temperature at 70 m in the SEIO. A positive correlation appears between the observed thermocline depth and subsurface temperature. We hereby denote R(Te, D) as a thermocline-subsurface temperature coupling coefficient, which can be measured by the slope in Figure 11. The observed slope is 0.1 K m-1, implying that one meter thermocline change would lead to a subsurface temperature change of 0.1K. All of the CMIP5 models reproduce such a positive relationship, even though the slope is markedly different. The comparison of the strong versus the weak composite shows that the thermocline-subsurface temperature feedback in the former is about 10% greater than that in the latter.

Figure 12 shows the averaged values of the SST-wind, wind-thermocline and thermocline-subsurface temperature coupling coefficients and BFI respectively for the strong, moderate and weak composites. For comparison, the observed coupling coefficients and BFI are also shown in the figure.

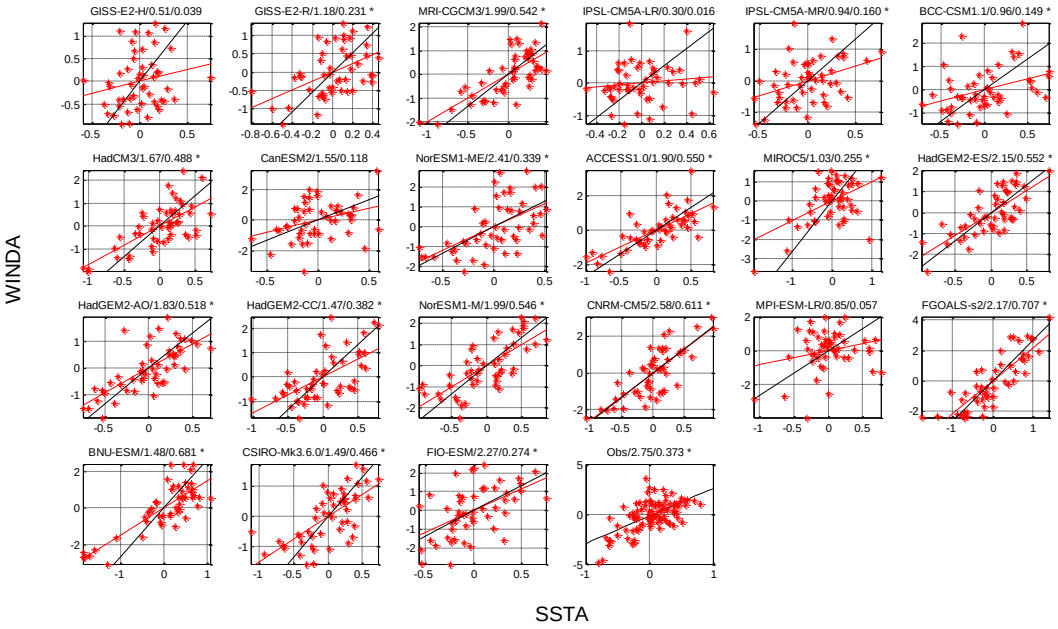

Figure. 9. Scatter diagrams revealing relationships between surface zonal wind anomaly (vertical axis, unit: m s-1) in the CEIO and SSTA (horizontal axis, unit: K) in the SEIO during the IOD developing phase (JAS) for each of 21 models (red). At each panel, the name of each model is shown in the top, and the numbers at the top indicate the slope of each fitted line and R2 between variables, the black line indicates the fitted line from observation, the asterisk indicates the model with significant relationship.

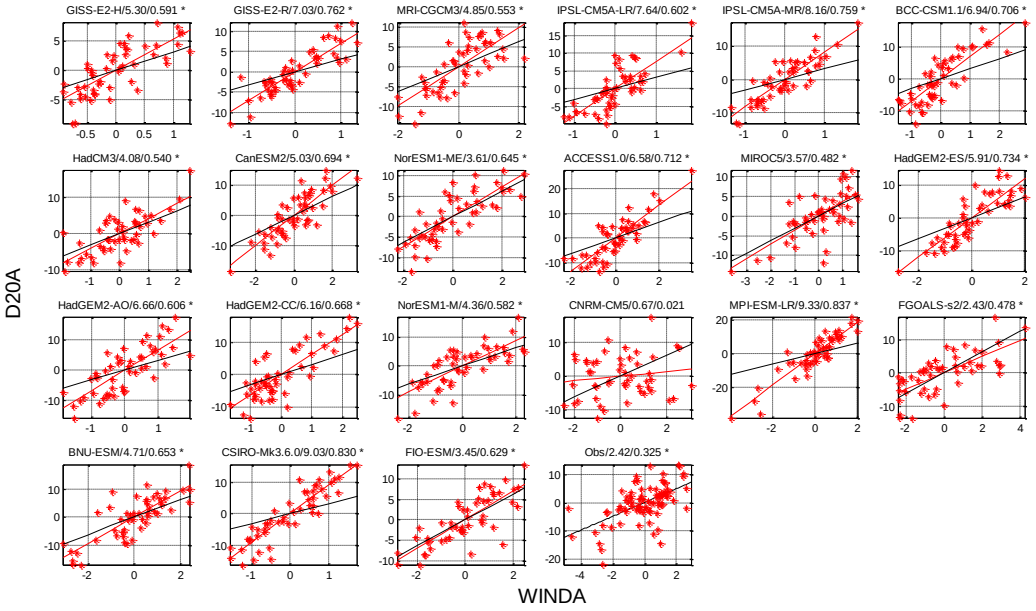

Figure. 10. Same as in Fig. 9 except for the relationship between the thermocline depth anomaly (vertical axis, unit: m) in the SEIO and the surface zonal wind anomaly (horizontal axis, unit: m s-1) in the CEIO.

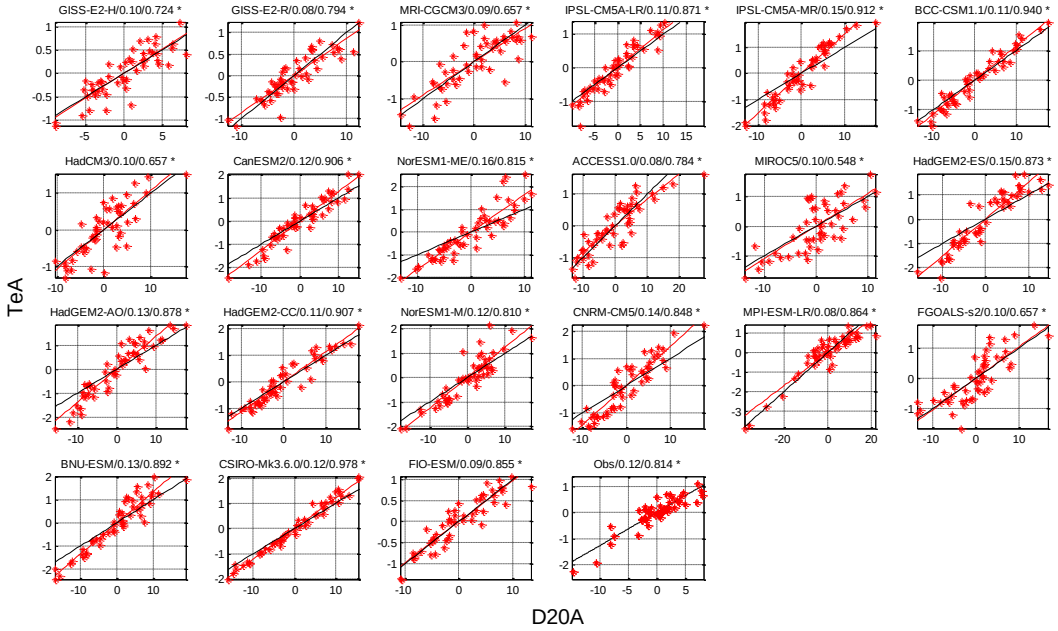

Figure 11. Same as in Fig. 9 except for the relationship between the subsurface temperature anomaly at 70 meters (vertical axis, unit: K) and the thermocline depth anomaly (horizontal axis, unit: m) in the SEIO.

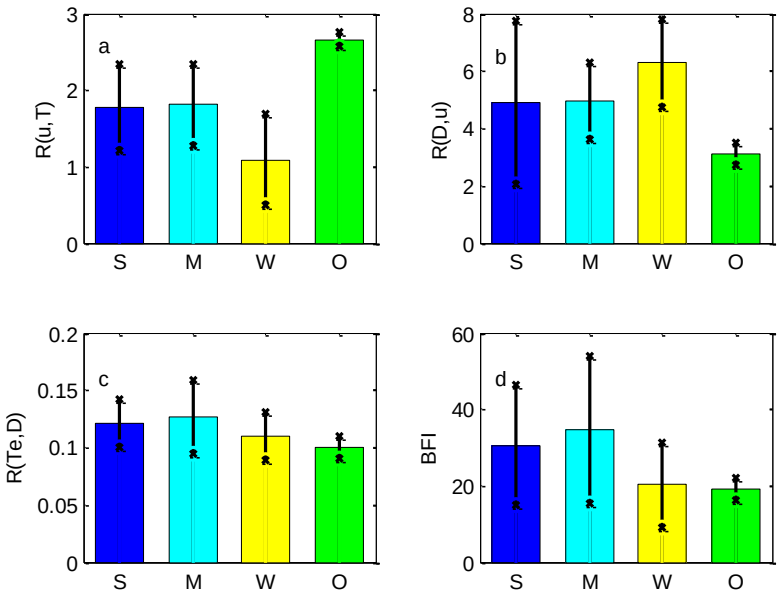

Figure 12. R(u,T) (unit: m s-1 k-1), R(D,u) (unit: m per m s-1), R(Te,D) (unit: K m-1) and BFI (unit: W m-2 K-1) in JAS season for the strong (denoted by 'S'), moderate (denoted by 'M'), and weak (denoted by 'W') composites and from the observational data (denoted by 'O'). Error bars indicate the strength spread among different groups.

b) Thermodynamic feedback

We hereby denote R(LHF, T) to represent the WES feedback coefficient, which can be measured by the slope at each panel of Fig. 13. The observed feedback coefficient is 4.17 W m-2 K-1. This amount of anomalous heat flux could be used to further enhance the local SST cooling. Many CMIP5 models (including these in the strong simulation group) fail to reproduce such a positive feedback process. The further study illustrates the unrealistic simulated latent heat flux feedback is due to the incorrect simulation of the surface wind speed field in the individual models. The result is similar with the CMIP3 coupled models (Liu et al. 2011). The large bias in the WES feedback poses a great challenge to many state-of-art CGCMs.

To examine the cloud-radiation-SST feedback among the 21 models, we show the simultaneous relationship between the shortwave radiation and SST anomalies averaged in JAS over the SEIO (Figure 14). Different from the positive WES feedback, a negative feedback between the observed SST and shortwave radiation anomalies exists in the SEIO. While most of the coupled models reproduce such a negative feedback process, HadCM3 model, surprisingly, exhibits a weak positive feedback.

We denote R(SWR, T) to measure the strength of the negative cloud-radiation-SST feedback. The averaged slope of the strong composite is -19 W m-2 K-1, which is about twice as large as that (-7.4 W m-2 K-1) in the weak composite.

Figure 15 shows the diagrams of R(LHF, T), R(SWR, T) and TFI for the strong, moderate and weak composites and for the observation. The major bias appears in the latent heat flux-SST relationship. Consequently, the overall thermodynamic damping in all the three groups

is overestimated, compared to the observation. The strongest (weakest) thermodynamic damping appears in the moderate (weak) group.

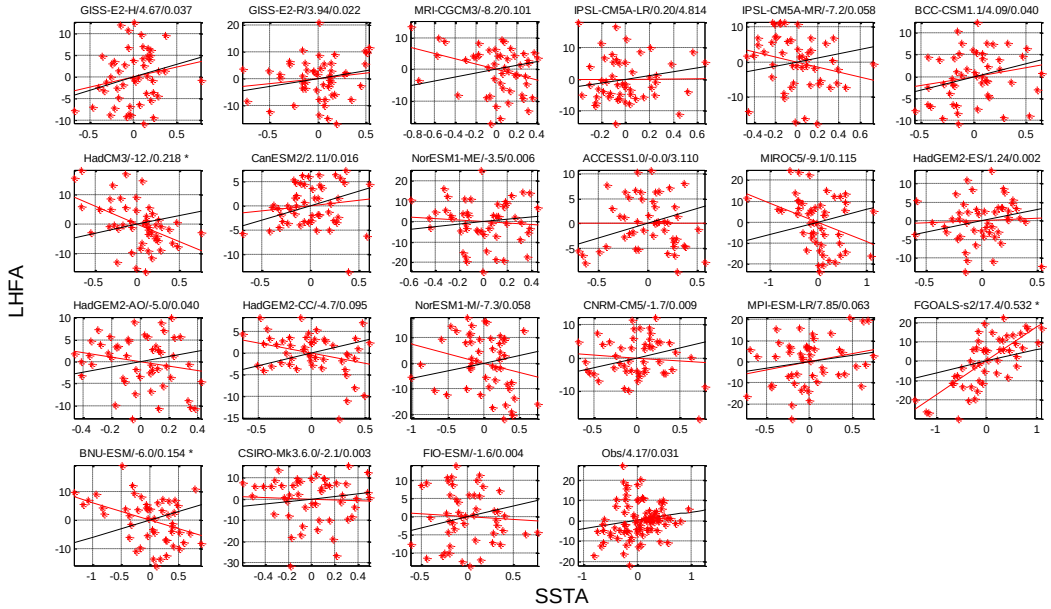

Figure 13. Similar as in Fig. 9 except for the relationship between the surface latent heat flux anomaly (vertical axis, unit: W m-2) and SSTA (horizontal axis, unit: K) in the SEIO on JJA season. The latent heat flux is defined positive downward.

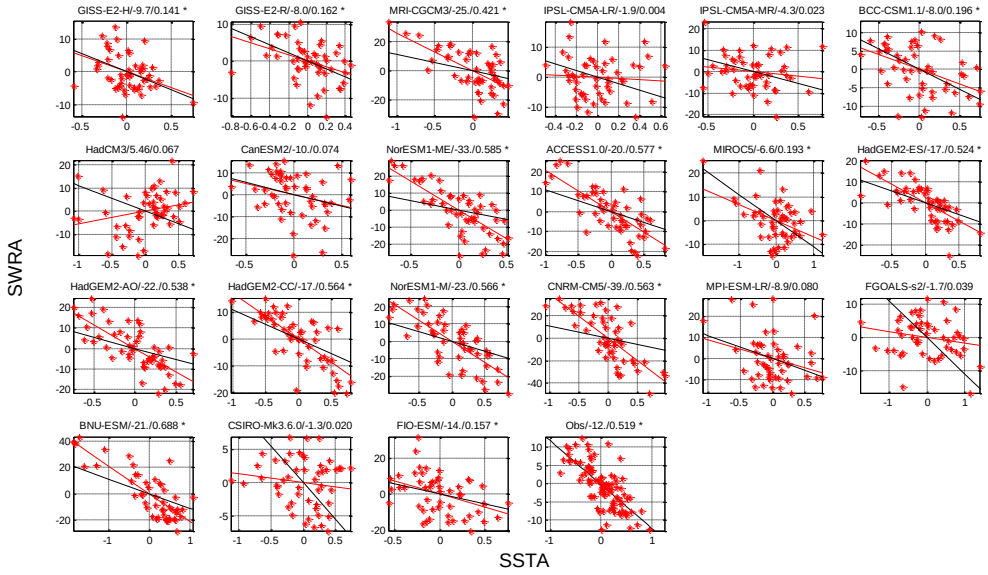

Figure 14. Same as in Fig. 9 except for the relationship between the surface net shortwave radiation anomaly (vertical axis, unit: W m-2) and SSTA (horizontal axis, unit: K) in the SEIO.

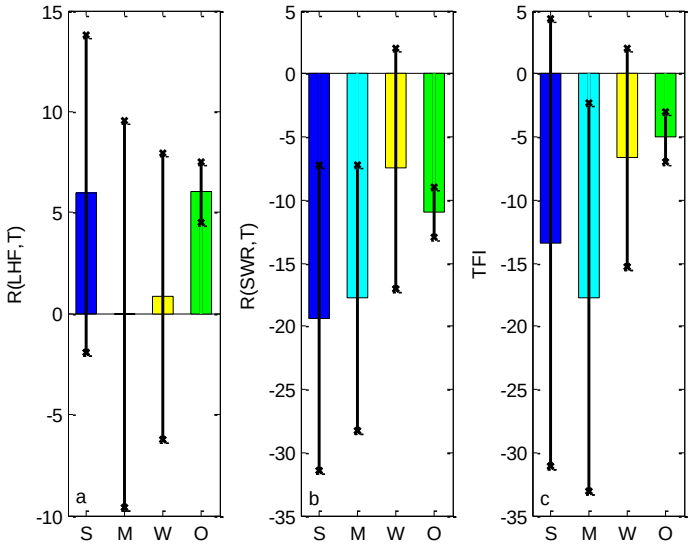

Figure 15. R(LHF,T), R(SWR,T) and TFI (unit: W m-2 K-1) averaged during JAS season for the strong, moderate and weak composites (denoted as 'S', 'M' and 'W' respectively) and from the observation (denoted as 'O'). Error bars indicate the strength spread among different groups.

c) Dissusion

Although most CMIP5 coupled models simulate the IOD mode and relevant dynamic and thermodynamic feedback processes in the tropical IO, unrealistic simulations exist among these models. The negative shortwave radiation-SST feedback is the important thermodynamic air-sea coupling process that could impact the IOD strength, which can be well captured by most of the CMIP5 models. However, the HadCM3 model fails to reproduce the observed feature.

The results point to possible biases in the thermodynamic air-sea coupling in some of current state-of-art CGCMs. The comparison of overall performance of the IOD simulations among the 21 models suggests that the most serious problem lies in the thermodynamic air-sea coupling. As most of these CGCMs are also used for future climate projection, caution is needed in interpreting the model generated global and regional SST changes.

3.2 Global Warming condition

Since the datasets of ocean temperature profiles are not able to be downloaded due to some reasons, we have to utilize the other method to measure the feedback mechanism for IOD event under global warming condition.

Since SST variability in the eastern EIO is highly correlated with the IOD index (Saji et al. 1999) based on the west-east SST difference, we calculate the standard deviation of the eastern EIO SST index during SON. The IOD intensity change shows some diversity among the models, but the ensemble mean changes vary little from 0.6 ^{o}C in 1950-2000 to 0.58 ^{o}C in 2045-2095. IOD strengthens in 7 models and weakens in the other 10 models. The inter-model standard deviation of the change is 0.13 ^{o}C, indicating uncertainties among the

models. In general, the SST activity remains unchanged under global warming in the ensemble mean over tropical Indian Ocean.

a) Dynamic feedback

As the mean thermocline shoals along with the weakened Walker circulation under global warming, the variations of the thermocline depth and upwelling affect SST variability more effectively. Figure 16a shows that the thermocline feedback parameter R(SST,D) increases in most models. The ensemble mean value rises from 11.3 ^{o}C/m in 1950-2000 to 13.4 ^{o}C/m in 2045-2095 by about 18%. In only 3 models (GFDL-ESM2G, INMCM4 and NorESM1-M) R(SST,D) decreases in a warmer climate. The uncertainty of the change among the models is about 2.2 ^{o}C/m, close to the ensemble mean change. The time series of R(SST,D) supports the thermocline feedback increase under global warming (Fig. 16c), but the feedback change shows some variations among models and low frequency natural modulations.

The strengthening of thermocline feedback is due to the thermocline shoaling in the eastern EIO. Figure 16b illustrates the relationship of thermocline feedback change, which is represented by the ratio of R(SST,D) in 2045-2095 to 1950-2000, with that of the mean thermocline depth. There is a significant negative correlation (r=-0.49): if the thermocline in the eastern EIO shoals more (less) in a coupled model than the ensemble mean, the thermocline feedback is more (less) enhanced. The thermocline feedback change also shows a high correlation (r=-0.56) with the zonal wind change in the eastern EIO. These results suggest that the uncertainty of the IOD oceanic feedback change under global warming is due to the diversity in thermocline change.

b) Thermodynamic feedback

Despite the shoaling thermocline and strengthened thermocline feedback, the interannual variance decreases under global warming in the thermocline depth, zonal wind and precipitation, indicating a weakened atmosphere response to IOD SST.

Zheng et al. (2010) hypothesized that the atmospheric component of Bjerknes feedback weakens under global warming due to the increased atmospheric dry static stability in the troposphere, the latter a robust feature of atmospheric change. We use the zonal wind feedback parameter R(U,T) to evaluate the atmospheric component of Bjerknes feedback. The scatter plot in Figure 17a compares R(U,T) in the 20th and 21st centuries. A pronounced decline in R(U,T) is found indicating the weakened zonal wind feedback. Only three models (CSIRO-Mk3.6.0, INM-CM4 and MIROC5) simulate a strengthened R(U,T). The ensemble mean value decreases from 2.1 m s-1 (oC) -1 to ~ 1.7 m s-1 (oC) -1. The variance of inter-model R(U,T) changes is 0.42 m s-1 (oC) -1, representing some discrepancy of the atmospheric response among the models. The time series of R(U,T) illustrate the decreasing trend, with some inter-model diversity and low frequency natural modulations (Fig. 17b).

Furthermore, to investigate the nature of weakened atmospheric IOD feedback, we perform a decomposition of R(U,T) into two parts: the regression of precipitation upon SST anomalies, R(Precip, T) in the eastern EIO, representing the precipitation response to SST anomalies; the regression of zonal wind upon precipitation anomalies, R(U, Precip), representing the zonal wind response to precipitation anomalies, the latter representing the atmospheric response to a heating source. Both of them are reduced in the 21st century but the ensemble mean changes are within the inter-model variance (Fig. 18). R(Precip, T)

weakens in 11 of 17 models with the ensemble mean decreasing from ~ 98 (mm mon-1)/oC to ~ 83 (mm mon-1)/oC. R(U, Precip) decreases in 13 of 17 models, with the ensemble mean changing from 0.02 (m s-1)/ (mm mon-1) to 0.0175 (m s-1)/ (mm mon-1). The latter index represents the atmospheric circulation response to anomalous heat source, related to the tropospheric stability. Zheng et al. (2010) emphasized that this term is important for the weakened atmospheric feedback, but the decreased R(Precip, T) also contributes to the weakened atmospheric feedback. We consider the possible mechanism of the weakened precipitation response. In the eastern EIO region, mean precipitation decreases following the "warmer-get-wetter" mechanism of Xie et al. (2010). The decrease of mean rainfall relative to the current climatology weakens interannual precipitation variability. The above-mentioned factors (circulation response to latent heating and precipitation response to SST) both cause the atmospheric feedback to weaken, counteracting the enhanced thermocline feedback.

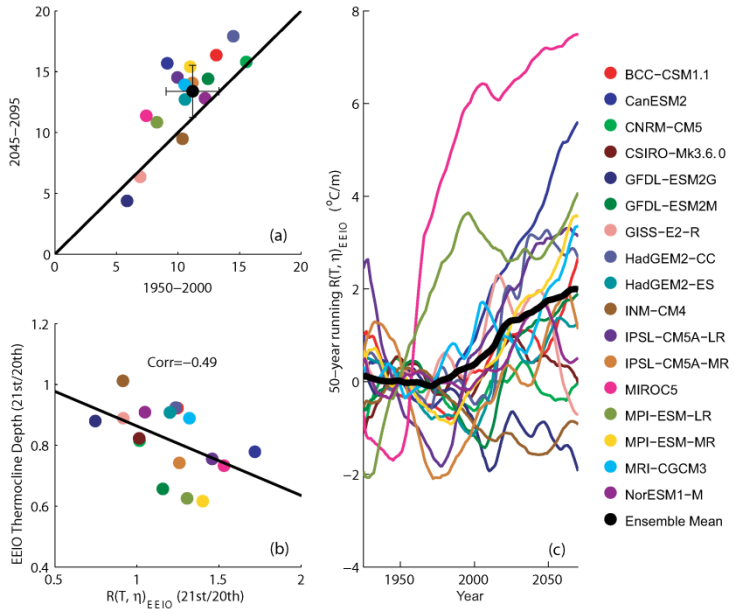

Figure16.(a) The scatter plots of R(SST,D oC/m) between 1950-2000 and 2045-2095. The black dot and errorbars denote the ensemble mean and standard deviation of inter-model variability, respectively. (b) The scatter plots of R(SST,D and thermocline depth ratios between 1950-2000 and 2045-2095. The solid line denotes the linear regression. (c) 50-year running time series of R(SST,D oC/m) for SON in 17 CMIP5 CGCMs referenced to the regression during 1901-2000. The black thick line is multi-model ensemble mean.

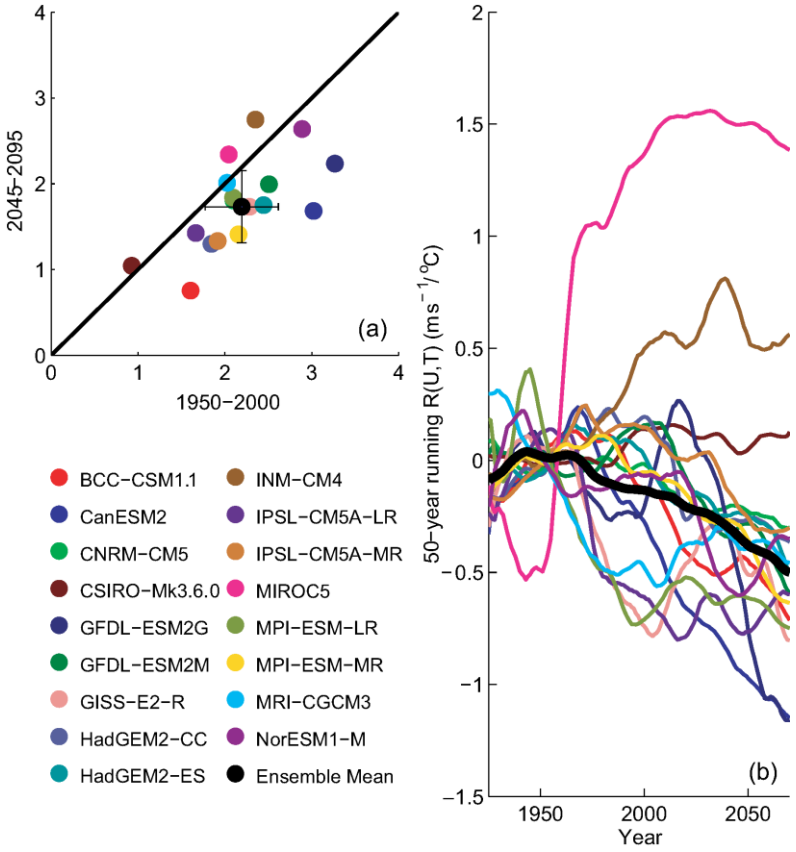

Figure 17. (a) The scatter plots of R(U,T m s-1 oC-1) between 1950-2000 and 2045-2095. The black dot and error bars denote the ensemble mean and standard deviation of inter-model variability, respectively. MIROC5 is excluded from ensemble mean calculation. (b) 50-year running time series of R(U,T m s-1 oC-1) for SON in 17 CMIP5 CGCMs referenced to the regression during 1901-2000. The black thick line is multi-model ensemble mean.

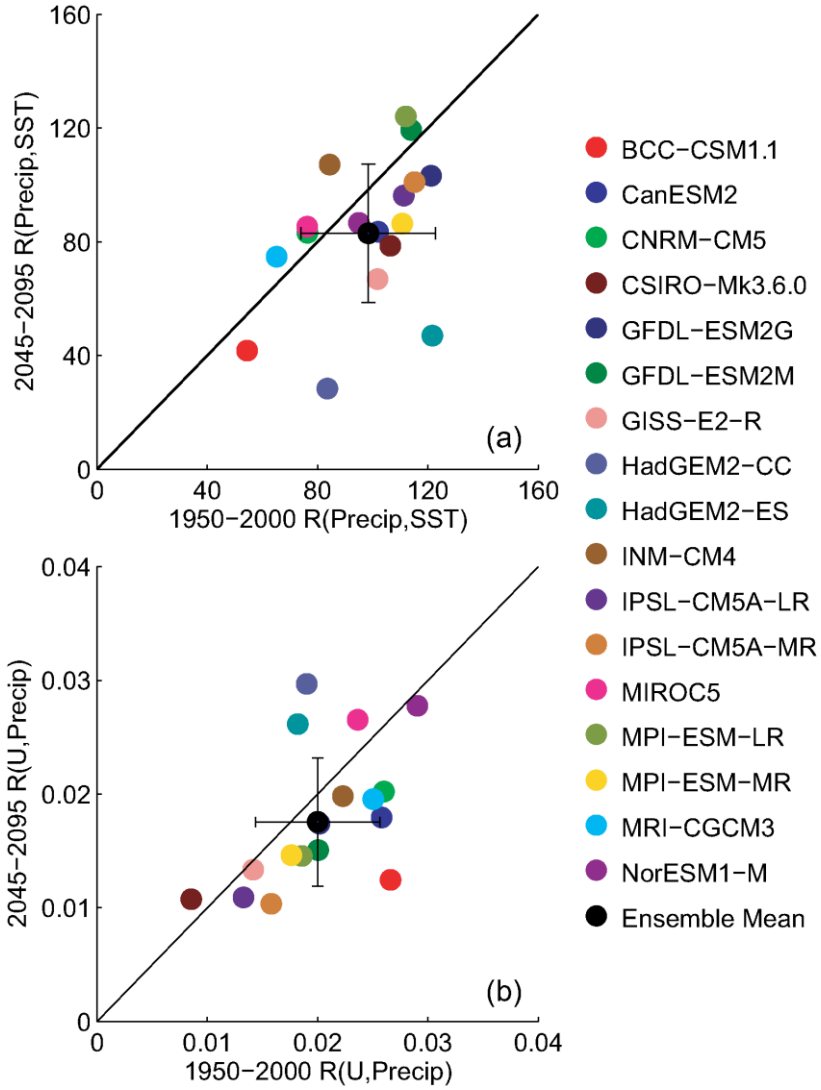

Figure 18. The scatter plots of standard deviations of (a) R(Precip,T) (mm mon-1 /oC) and (b) R(U,Precip) (m s-1/mm mon-1) between 1950-2000 and 2045-2095. The black dot and error bars denote the ensemble mean and standard deviation of inter-model variability, respectively. MIROC5 is excluded from ensemble mean calculation.

C) Discussion

In global warming, the ensemble mean thermocline in the eastern EIO shoals, which lead to a weakened Walker circulation and easterly wind change along the equator, along with a dipole-like pattern of SST/precipitation change. The inter-model variability in changes of SST, zonal wind and thermocline depth are highly correlated with each other, indicating the close coupling of ocean-atmosphere fields in TIO.

The mean state change affects the interannual IOD mode, although the ensemble mean IOD variance in SST does not change much under global warming, with some diversity among the models. The shoaling thermocline in the eastern EIO leads to a strengthened thermocline feedback, enabling subsurface temperature anomalies to affect SST more effectively. The strengthening of thermocline feedback, however, does not lead to an intensification of IOD. The atmospheric response weakens, counteracting the stronger thermocline feedback due to a shoaling thermocline. Our decomposition analysis of zonal

wind feedback shows that the increased tropospheric stability and reduced interannual variability of precipitation in the eastern EIO are both the reasons for the weakened atmospheric feedback.

4. Conclusions

The Indian Ocean Dipole is one of dominant modes in the tropical IO on the interannual timescale. This study shows that the simulated IOD in CMIP5 has not improved much compared to CMIP3. Although the ensemble averaged IOD strength in CMIP5 is closer to observations. In this study we evaluate the performance of 21 WCRP CMIP5 models in IOD simulation, by examining the dynamical and thermodynamic air-sea coupling processes.

To study the cause of the diversity in the model IOD intensity, we first examine the Bjerknes feedback. This dynamic ocean-atmosphere feedback consists of the following three key processes: 1) how strongly the atmospheric low-level wind responds to one unit SSTA forcing, 2) how strongly the ocean thermocline depth responds to one unit surface wind forcing, and 3) how strongly the ocean subsurface temperature responds to one unit thermocline depth variation. These three dynamical feedback processes are examined and the respective coupling coefficients are estimated in all the 21 models. The overall strength of the Bjerknes dynamic feedback is determined by the product of the three coupling coefficients and the mean upwelling velocity. The comparison of the strong and weak composites shows that the former attains a much greater Bjerknes feedback intensity than the latter.

Next we examine the thermodynamic air-sea coupling strength for all the 21 models. Two thermodynamic air-sea feedback processes, WES feedback and the cloud-radiation-SST feedback, are examined. While observations show a positive feedback among the wind, evaporation (or surface latent heat flux) and SST during the IOD developing phase, about a half of the CMIP5 models failed to capture this thermodynamic air-sea feedback. As a strong negative feedback process, the cloud-radiation-SST feedback may slow down the IOD development. Most of the CMIP5 models successfully simulated this negative feedback process, even though the feedback intensity varies among the models. The averaged negative feedback coefficient is greater (smaller) in the strong (weak) composite than observation, implying a stronger (weaker) thermodynamic damping.

The CMIP5 ensemble produces a more realistic positive WES feedback during the IOD developing phase, while it produces a worse Bjerknes dynamic feedback than CMIP3. The lack in improvement from CMIP3 to CMIP5 is most noticeable in the wind response to SST forcing which is underestimated in the newer generation models while the thermocline response to surface wind forcing is overestimated. The overall CMIP5 performance in the IOD simulation does not show remarkable improvement compared to the CMIP3 simulations.

The distinctive features in the dynamic and thermodynamic coupling between the strong and weak composite are closely related to the difference in the coupled model mean state. The comparison of the strong and weak composites shows that there are remarkable differences in the mean thermocline depth. The models with a deeper mean thermocline are often associated with weaker dynamic coupling strength and a weak IOD signal.

We have also investigated the IOD response to global warming and the related mean state change based on historical simulations and future climate projections by 17 CMIP5 models. In global warming, the ensemble mean thermocline in the eastern EIO shoals by about 15 m. This shoaling thermocline is a result of a weakened Walker circulation and easterly wind change along the equator, along with a dipole-like pattern of SST/precipitation change. The inter-model variability in changes of SST, zonal wind and thermocline depth are highly correlated with each other, indicating the close coupling of ocean-atmosphere fields in TIO.

The mean state change affects the interannual IOD mode, although the ensemble mean IOD variance in SST does not change much under global warming, with some diversity among the models. The shoaling thermocline in the eastern EIO leads to a strengthened thermocline feedback, enabling subsurface temperature anomalies to affect SST more effectively. The strengthening of thermocline feedback, however, does not lead to an intensification of IOD. The atmospheric response weakens, counteracting the stronger thermocline feedback due to a shoaling thermocline. Our decomposition analysis of zonal wind feedback shows that the increased tropospheric stability and reduced interannual variability of precipitation in the eastern EIO are both the reasons for the weakened atmospheric feedback.

5. Future Directions

In global warming condition, the proposed research had been modified due to the limited data downloading issue. In the future, we are going to continue the data preparation for the further analysis based on the methodology introduced in Section 2.

Previous sections describe the detailed information for the scientific research, but the relevant communication among different projects and other international associations will be the most important activities we should strengthen in the future. As we mentioned before, the project outcome presents the importance of the upwelling for IOD simulation, which is also one of the major concern of CLIVAR as upwelling is one of the research foci in the future for CLIVAR level. Based on our finding, EIOURI project invited the participants of this project to join and contribute to IIOE-2 in the quite near future.

After the communication and discussion with the representative, the pilot project of IOC/WESTPAC, MOMSEI, has agreed to work together, which will be a good opportunity for disseminating our project into more persons and organization. The proponents will try the best to enhance the communication with IOC/WESTPAC for the further cooperation. Also, we will build the connection with numerical model developer in order to improve their coupled models based on our research.

References

Carton, J. A., G. Chepurin, X. Cao, and B. Giese, 2000: A simple ocean data assimilation analysis of the global upper ocean 1950–95. Part I: Methodology. J. Phys. Oceanogr., 30, 294–309.

Gill, A. E., 1980: Some simple solutions for heat-induced tropical circulation. Quart. J. Roy. Meteor. Soc., 106, 447–462.

Hong, C.-C., and T. Li, 2010: Independence of SST skewness from thermocline feedback in the eastern equatorial Indian Ocean, Geophys. Res. Lett., 37, L11702, doi:10.1029/2010GL043380.

Kistler, R., E. Kalnay, W. Collins, S. Saha, G. White, J. Woollen, M. Chelliah, W. Ebisuzaki, M. Kanamitsu, V. Kousky, H. van den Dool, R. Jenne, and M. Fiorino, 2001: The NCEP-NCAR 50-Year Reanalysis: Monthly Means CD-ROM and Documentation. Bull. Amer. Meteor. Soc., 82, 247–268.

Li, T., Y. S. Zhang, E. Lu, and D. Wang, 2002: Relative role of dynamic and thermodynamic processes in the development of the Indian Ocean dipole. Geophy. Res. Let., 29, 2110–2113.

Li, T., B. Wang, C.-P. Chang, and Y. Zhang, 2003: A theory for the Indian Ocean dipole-zonal mode. J. Atmos. Sci., 60, 2119–2135.

Lindzen, R. S. and S. Nigam, 1987: On the role of sea surface temperature gradients in forcing low level winds and convergence in the tropics. J. Atmos. Sci., 44, 2418–2436.

Liu L., W. Yu and T. Li, 2011: Dynamic and Thermodynamic Air–Sea Coupling Associated with the Indian Ocean Dipole Diagnosed from 23 WCRP CMIP3 Models. Journal of Climate, 24, 4941-4958.

Neelin, J. D., 1991: The slow sea surface temperature mode and the fast-wave limit: Analytic theory for tropical interannual oscillations and experiments in a hybrid coupled model. J. Atmos. Sci., 48, 584–606.

Rayner, N. A., D. E. Parker, E. B. Horton, C. K. Folland, L. V. Alexander, D. P. Rowell, E. C. Kent and A. Kaplan, 2003: Global analyses of sea surface temperature, sea ice, and night marine air temperature since the late nineteenth century. J. Geophys. Res., 108, No. D14, 4407 10.1029/2002JD002670.

Saji, N. H., B. N. Goswami, P. N. Vinayachandran, and T. Yamagata, 1999: A dipole mode in the tropical Indian Ocean. Nature, 401, 360–363.

Taylor, K.E., R.J. Stouffer, G.A. Meehl, 2012: An Overview of CMIP5 and the experiment design.” Bull. Amer. Meteor. Soc., 93, 485-498, doi:10.1175/BAMS-D-11-00094.1

Yu, W., B. Xiang, L. Liu and N. Liu, 2005: Understanding the origins of interannual thermocline variations in the tropical Indian Ocean. Geophys. Res. Lett., 32, L24706, doi:10.1029/2005GL024327.

Xie, S.-P., C. Deser, G.A. Vecchi, J. Ma, H. Teng, and A.T. Wittenberg, 2010: Global warming pattern formation: Sea surface temperature and rainfall. J. Climate, 23, 966-986.

Zheng, X.-T., S.-P. Xie, G.A. Vecchi, Q. Liu, and J. Hafner, 2010: Indian Ocean dipole response to global warming: Analysis of ocean-atmospheric feedbacks in a coupled model. J. Climate, 23, 1240–1253.

Appendix

Conferences/Symposia/Workshops

Agenda for

"The Impact of Global Warming on Ocean-Atmosphere Feedback Strength at the Tropical Indian Ocean" Workshop

15-17 August 2014

Chengdu, China

Time	Programs
15 August 2014	
	Registration
16 August 2014	**Workshop**
09:00-09:10	Opening Session
	Welcome address and Opening address Dr. Lin Liu, FIO,SOA, China
Time	Session 1: Progress of the Project Chairs: Dr. Tim Li
09:10-09:20	The introduction of the APN project and the relevant progress Dr. Lin Liu, FIO
09:20-10:00	Global warming impact on ENSO amplitude Prof. Tim Li, IPRC
10:00-10:30	CMIP5 data analysis over the Southeast Asian Maritime Continent Dr. Juneng Liew, UKM
10:30-10:40	Group Photo and Coffee Break
10:40-11:10	The assessment of IOD event in CMIP5 models Dr. Lin Liu, FIO

11:40-12:10	Response of Marine Hazards to different El Nino event Dr. Xin Wang, SCSIO
12:10-14:00	Lunch Break
14:00-14:30	The Impact from IOD on the fishery off Java Dr. Anna, AMDRD
14:30-15:30	Discussion
15:30-15:40	Coffee Break
15:40-17:00	Discussion
18:00-20:00	Welcome banquet
17 August 2014	**Workshop**
09:00-12:00	Discussion
18 August 2014	**Departure**

Participants

Prof. Tim LI
International Pacific Research Center and Department of
Meteorology, School of Ocean and Earth Science and
Technology, University of Hawaii, Honolulu, Hawaii 96822
Phone: (808) 956-9427; Fax: (808) 956-9425
Email: timli@hawaii.edu

Dr. Anna Kuswardani,
Research and Development Center for Marine and Coastal Resources
Agency for Research and Development of Marine and Fisheries,
Ministry of Marine Affairs and Fisheries, Indonesia
Phone: +006 2811 232 994
Email: anastasia.tisiana@gmail.com

Dr. Juneng, LIEW
School of Environmental and Natural Resource Sciences
Faculty of Science and Technology
Universiti Kebangsaan Malaysia
43600, UKM Bangi
Selangor D.E.
Malaysia
Phone: +60 172 125151

Email: jnliew@gmail.com

Prof. Xin WANG
South China Sea Institute of Oceanography
No. 164, Rd. Xin-Gang-XI, Guangzhou, China
Phone: 020-34134191; FAX: 020-34134191
Email: wangxin@scsio.ac.cn

Dr Lin LIU
Center for Ocean and Climate Research
The First Institute of Oceanography, State Oceanic Administration
No.6 Xian-Xia-Ling Road, High-Tech Park
Qingdao 266061, P.R.CHINA
Tel : +86-(0)532-88961173; Fax: +86-(0)532-88961173
Email : liul@fio.org.cn;

Ms. Laoyu LI
Project officer of MOMSEI project
Center for Ocean and Climate Research
The First Institute of Oceanography, State Oceanic Administration
No.6 Xian-Xia-Ling Road, High-Tech Park
Qingdao 266061, P.R.CHINA
Tel : +86-(0)532-88960673; Fax: +86-(0)532-88960673
Email : lilaoyu@fio.org.cn;

Mr. Jianjun LIU
Center for Ocean and Climate Research
The First Institute of Oceanography, State Oceanic Administration
No.6 Xian-Xia-Ling Road, High-Tech Park
Qingdao 266061, P.R.CHINA
Tel : +86-(0)532-88967403; Fax: +86-(0)532-88967403
Email : lijj@fio.org.cn;

Ms. Ke AN
Center for Ocean and Climate Research
The First Institute of Oceanography, State Oceanic Administration
No.6 Xian-Xia-Ling Road, High-Tech Park
Qingdao 266061, P.R.CHINA
Tel : +86-(0)532-88961173; Fax: +86-(0)532-88961173
Email : anke@fio.org.cn;

Abstract of the presentation

Funding sources outside the APN

1. National Science Foundation of China (NSFC, Non-governmental agency)
   The project leader had been sponsored by NSFC from 2014 to 2017, which provide around $ 6,000 US dollars for the project leader to participant the 1st Pan-CLIVAR meeting at Hague. Also, NSFC co-support this project for the next 2 years.

2. IOC/WESTPAC (Inter-governmental agency)
   The pilot project MOMSEI provides around $4000 for the project to join the summer school in Jakarta and also is agreed to cooperate with this project in upwelling issues.

3. Ocean University of China (OUC, non-government agency)
   OUC provides the data download convenience for this project. More than 60% CMIP5 data was provided by OUC server.

List of Young Scientists

None

Glossary of Terms

Full name	Acronyms
Intergovernmental Oceanographic Commission /Sub-Commission for the Western Pacific	IOC/WESTPAC
Indian Ocean Dipole	IOD
Monsoon Onset Monitoring and its Social Economy Impact	MOMSEI
The Java Upwelling dynamic and the relevant ecosystem variation	JUV
World Climate Research Programme	WCRP
Climate Variability and Predictability	CLIVAR
Coupled Model Intercomparison Project	CMIP
Wind-Evaporation-Sea surface temperature	WES
July-August-September	JAS
Intergovernmental Panel on Climate Change Fifth Assessment Report	IPCC AR5